

1 *Research Article – Journal of Neuroscience*

2 **Activation of extrasynaptic kainate receptors drives hilar mossy cell activity**

3 Abbreviated title: Extrasynaptic KARs in mossy cells

4 Czarina Ramos^{1*}, Stefano Lutz^{1*}, Miwako Yamasaki², Yuchio Yanagawa³, Kenji Sakimura⁴, Susumu
5 Tomita⁵, Masahiko Watanabe² and Pablo E. Castillo^{1,6‡}

6

7 ¹Dominick P. Purpura Department of Neuroscience Albert Einstein College of Medicine, 1300 Morris
8 Park Avenue Bronx, NY, 10461, USA.

9 ²Department of Anatomy, Faculty of Medicine, Hokkaido University, Sapporo 060-8638, Japan.

10 ³Department of Genetic and Behavioral Neuroscience, Gunma University Graduate School of
11 Medicine, Maebashi 371-8511, Japan.

12 ⁴Department of Cellular Neurobiology, Brain Research Institute, Niigata University, Niigata 951-
13 8585, Japan.

14 ⁵Department of Cellular and Molecular Physiology, Department of Neuroscience, and Kavli Institute
15 for Neuroscience, Yale University School of Medicine, New Haven, Connecticut 06520, USA.

16 ⁶Department of Psychiatry and Behavioral Sciences, Albert Einstein College of Medicine, 1300
17 Morris Park Avenue Bronx, NY, 10461, USA.

18

19 * These authors contributed equally to this work.

20 ‡ To whom correspondence should be addressed:

21 Pablo E. Castillo, MD/PhD
22 Dominick P. Purpura Department of Neuroscience
23 Albert Einstein College of Medicine
24 1410 Pelham Parkway South
25 Kennedy Center, Room 703
26 Bronx, NY 10461, USA
27 Email: pablo.castillo@einsteinmed.org

28

29

30 The authors declare no conflict of interest.

31

32 **Acknowledgments:** We thank the members of the Castillo lab (in particular Dr. Kaoutsar Nasrallah) for
33 constructive feedback and for reading and commenting the manuscript. This research was supported
34 by the National Institutes of Health: R01-NS113600, R01-MH116673 and R01MH125772 to P.E.C;
35 Grant-in-Aid for Specially Promoted Research from Japan Society for the Promotion of Science (JSPS)
36 (20H05628) and for Scientific Research B from Japan Society for the Promotion of Science (JSPS)
37 (21H02589) to M.W.; JSPS KAKENHI Grants (17H0631310 and 20H03410) to M.Y.

38 Number of pages: 24

39 Number of figures: 6

40 Number of words: Abstract (241), Introduction (699) and Discussion (1,317)

41

1 **Abstract:**

2 Mossy cells (MCs) of the dentate gyrus (DG) are key components of an excitatory associative
3 circuit established by reciprocal connections with dentate granule cells (GCs). MCs are implicated
4 in place field encoding, pattern separation and novelty detection, as well as in brain disorders
5 such as temporal lobe epilepsy and depression. Despite their functional relevance, little is known
6 about the determinants that control MC activity. Here, we examined whether MCs express
7 functional kainate receptors (KARs), a subtype of glutamate receptors involved in neuronal
8 development, synaptic transmission and epilepsy. Using mouse hippocampal slices, we found
9 that bath application of submicromolar and micromolar concentrations of the KAR agonist kainic
10 acid induced inward currents and robust MC firing. These effects were abolished in *GluK2* KO
11 mice, indicating the presence of functional GluK2-containing KARs in MCs. In contrast to CA3
12 pyramidal cells, which are structurally and functionally similar to MCs, and express synaptic KARs
13 at mossy fiber (MF) inputs (i.e., GC axons), we found no evidence for KAR-mediated transmission
14 at MF-MC synapses, indicating that most KARs at MCs are extrasynaptic. Immunofluorescence
15 and immunoelectron microscopy analyses confirmed the extrasynaptic localization of GluK2-
16 containing KARs in MCs. Finally, blocking glutamate transporters, a manipulation that increases
17 extracellular levels of endogenous glutamate, was sufficient to induce KAR-mediated inward
18 currents in MCs, suggesting that MC-KARs can be activated by increases in ambient glutamate.
19 Our findings provide the first direct evidence of functional extrasynaptic KARs at a critical
20 excitatory neuron of the hippocampus.

21

22 **Significance Statement:**

23 Hilar mossy cells (MCs) are an understudied population of hippocampal neurons that form an
24 excitatory loop with dentate granule cells. MCs have been implicated in pattern separation, spatial
25 navigation, and epilepsy. Despite their importance in hippocampal function and disease, little is
26 known about how MC activity is recruited. Here, we show for the first time that MCs express
27 extrasynaptic kainate receptors (KARs), a subtype of glutamate receptors critically involved in
28 neuronal function and epilepsy. While we found no evidence for synaptic KARs in MCs, KAR
29 activation induced strong action potential firing of MCs, raising the possibility that extracellular
30 KARs regulate MC excitability *in vivo* and may also promote dentate gyrus hyperexcitability and
31 epileptogenesis.

32

1 Introduction

2 Hilar mossy cells (MCs) in the hilus of the dentate gyrus (DG) are major excitatory neurons that
3 widely project onto dentate granule cells (GCs) to control their activity (Buckmaster and
4 Schwartzkroin, 1994; Hashimoto et al., 2017; Scharfman, 2018; Botterill et al., 2019). Within
5 the DG, MCs form an associative network with GCs, in which MCs receive extensive convergent
6 excitatory inputs from GCs (Patton and McNaughton, 1995; Acsady et al., 1998; Buckmaster and
7 Jongen-Relo, 1999; Ribak and Shapiro, 2007) and then send excitatory feedback projections to
8 up to ~30,000 GCs along the dorsoventral axis of the ipsi- and contralateral hippocampus (Ribak
9 et al., 1985; Frotscher et al., 1991; Buckmaster et al., 1996; Wenzel et al., 1997). Thus, the activity
10 of a single MC can significantly impact the activity of numerous GCs, and ultimately, DG-CA3
11 information transfer. MCs contribute to hippocampal-dependent computations and behaviors
12 such as pattern separation, spatial navigation and other cognitive functions such as novelty
13 detection (Duffy et al., 2013; Danielson et al., 2017; GoodSmith et al., 2017; Senzai and Buzsaki,
14 2017; Fredes et al., 2021). In addition, aberrant MC function has been linked to brain disorders
15 such as temporal lobe epilepsy (TLE), depression, anxiety and schizophrenia (Scharfman, 2016).
16 Despite the important role that MCs play in brain function and disease, the mechanisms through
17 which MC activity is recruited are still largely unexplored.

18

19 MCs share many structural and functional properties with CA3 pyramidal cells. Both CA3
20 pyramidal cells and MCs receive in their proximal dendrites a major excitatory input from GCs via
21 the mossy fibers axons (MF), which impinge on complex spines called thorny excrescences (TEs)
22 via giant presynaptic boutons (Amaral and Dent, 1981; Acsady et al., 1998). Functionally, the MF-
23 to-MCs (MF-MC) synapse expresses robust forms of short- and long-term plasticity (Lysetskiy et
24 al., 2005), similar to those reported at the MF-to-CA3 pyramidal cell (MF-CA3) synapse (Henze
25 et al., 2002; Nicoll and Schmitz, 2005). In addition, glutamate release at both synapses is inhibited
26 by activation of presynaptic group 2/3 metabotropic glutamate receptors (mGluR2/3) (Kamiya et
27 al., 1996; Lysetskiy et al., 2005). While excitatory transmission is mainly mediated by AMPA and
28 NMDA ionotropic glutamate receptors, a slow component of MF-CA3 synaptic transmission is
29 mediated by kainate receptors (KARs) (Castillo et al., 1997). A similar, albeit modest KAR-
30 mediated component has recently been reported at the MF-MC synapse (Hedrick et al., 2017).
31 KARs are ionotropic glutamate receptors expressed in several brain areas, which have been
32 implicated in neuronal development, neuronal excitability, synaptic transmission and plasticity

1 (Lerma and Marques, 2013). *In vivo* injection of the KAR agonist kainic acid (KA), a widely used
2 animal model of TLE (Rusina et al., 2021), strongly activates CA3 pyramidal neurons (Westbrook
3 and Lothman, 1983; Crepel and Mulle, 2015), and also leads to extensive MCs loss (Buckmaster
4 and Jongen-Relo, 1999; Sloviter et al., 2003), suggesting that MCs are particularly sensitive to
5 the activation of KARs. Intriguingly, while KAR-mediated responses are much weaker at MF-MC
6 synapses (Hedrick et al., 2017) than at MF-CA3 synapses (Castillo et al., 1997; Mulle et al., 1998),
7 transcriptome profiling revealed that MCs and CA3 pyramidal cells display comparable levels of
8 transcripts for the functional KAR subunit GluK2 (Cembrowski et al., 2016), raising the possibility
9 that KARs may have additional roles at MCs.

10

11 In this study, we combined *in vitro* electrophysiology in acute rat and mouse hippocampal slices,
12 of wild type and *GluK2* knockout (KO) mice, with anatomical approaches such as
13 immunofluorescence and immunoelectron microscopy, to determine the role and subcellular
14 localization of KARs in MCs. We found that submicromolar and micromolar concentrations KA
15 induced robust inward currents and strong MC firing, and both effects were absent in *GluK2* KO
16 mice. Surprisingly, unlike in CA3 pyramidal neurons (Castillo et al., 1997), MF activation did not
17 elicit any measurable KAR-mediated synaptic response in MCs. Consistent with these
18 observations, immunofluorescence and immunoelectron microscopy revealed GluK2-containing
19 KARs in the soma and dendrites of MCs, but nearly absent from MC TEs. Lastly, blocking
20 glutamate uptake by excitatory amino-acid transporters (EAATs) elicited KAR-mediated inward
21 currents in MCs. Altogether, our findings support the notion that MCs express functional
22 extrasynaptic KARs whose activation by pharmacological agents (e.g., KA) and ambient
23 glutamate may play an important role in engaging the GC-MC-GC recurrent circuit.

24

25 **METHODS**

26 **Animals**

27 Experiments were performed on postnatal Sprague-Dawley rats (P18-P28) of both sexes and
28 C57BL/6 mice of both sexes for electrophysiological recordings. Animals were group-housed in a
29 standard 12h light/12h dark cycle. WT, *GluK2* KO, and *GAD67*^{+GFP} mice (Tamamaki et al., 2003);
30 were obtained from Dr. Yanagawa, Gunma University, Japan. Handling and use of animals
31 adhered to a protocol approved by the Animal Care and Use Committee at the Albert Einstein

1 College of Medicine, at Yale University and at the Faculty of Medicine at Hokkaido University and
2 in accordance with guidelines provided by the National Institutes of Health.

3

4 **Hippocampal Slice Preparation**

5 Animals were deeply anesthetized with isoflurane and then decapitated. The brain was then
6 rapidly removed from the skull and then hippocampi were dissected. Hippocampi were included
7 in agar supports and acute transverse hippocampal slices (400 μm thick for Sprague-Dawley rats,
8 300 μm for C57BL/6 mice) were cut using a VT1200s vibratome (Leica Microsystems Co.) in a
9 sucrose-based cutting solution containing (in mM): 215 sucrose, 2.5 KCl, 26 NaHCO_3 , 1.6
10 NaH_2PO_4 , 1 CaCl_2 , 4 MgCl_2 , 4 MgSO_4 , and 20 D-glucose. After 15 mins in recovery post-
11 sectioning, the solution was replaced by extracellular artificial cerebrospinal fluid (ACSF)
12 recording solution containing (in mM): 124 NaCl, 2.5 KCl, 26 NaHCO_3 , 1 NaH_2PO_4 , 2.5 CaCl_2 , 1.3
13 MgSO_4 , and 10 D-glucose. Slices were incubated for a minimum of 30 minutes in the ACSF before
14 recording. Solutions were equilibrated with 95% O_2 and 5% CO_2 (pH 7.4).

15

16 **Electrophysiology**

17 All experiments were performed in a submersion-type recording chamber perfused at $\sim 2 \text{ mL min}^{-1}$
18 1 , at $28 \pm 1^\circ\text{C}$, except those in **Fig. 6** where temperature was raised to $34^\circ\text{C} \pm 1^\circ\text{C}$. Whole-cell
19 patch clamp recordings using a Multiclamp 700A amplifier (Molecular Devices) were performed
20 from MCs and GCs in voltage-clamp ($V_{\text{hold}} -60 \text{ mV}$), or in current-clamp configuration ($V_{\text{rest}} \sim -65$
21 mV) using borosilicate pipette electrodes ($\sim 3\text{-}4 \text{ M}\Omega$). Recordings were performed using a K^+ -
22 based internal solution containing (in mM): 135 KMeSO_4 , 5 KCl, 1 CaCl_2 , 5 NaOH, 10 HEPES, 5
23 MgATP , 0.4 Na_3GTP , 5 EGTA, 10 D-glucose, pH 7.2 (280-290 mOsm). In some recordings we
24 also employed a Cs^+ -based internal solution containing (in mM): 131 Cs-gluconate, 8 NaCl, 1
25 CaCl_2 , 10 EGTA, 10 D-glucose and 10 HEPES, pH 7.2 (285-290 mOsm). Series resistance ($\sim 7\text{-}$
26 $25 \text{ M}\Omega$) was monitored throughout all experiments with a -5 mV , 80 ms voltage step, and cells
27 that exhibited a significant change ($>20\%$) were excluded from analysis.

28 MCs were identified using previously established criteria (Larimer and Strowbridge, 2008).
29 Specifically, we measured firing properties and membrane time constant by injection of a step of
30 depolarizing current while in current-clamp configuration. Cells were confirmed as MCs by
31 exhibiting elevated spontaneous synaptic activity, little to no afterhyperpolarization and non-burst

1 firing patterns upon depolarizing pulses (5s duration, 60-120 pA). Additional confirmation was
2 performed post-hoc through morphological analysis of biocytin-filled cells where MCs were
3 identified by the presence of distinctive complex TEs in their proximal dendrites. To isolate KAR-
4 mediated currents and EPSCs, we bath applied a cocktail of antagonists which included:
5 LY303070 (15 μ M) or GYKI 53655 (GYKI – 30 μ M) , D-APV (25 μ M), picrotoxin (50 μ M) and
6 CGP35348 (3 μ M) to block AMPA, NMDA, GABA_A and GABA_B receptors, respectively. The
7 cocktail was applied right after the target cell was identified as a MC. For the isolation of KAR-
8 EPSC, we first monitored AMPAR-EPSCs in presence of the above specified cocktail, without
9 LY303070, which was bath applied after a stable baseline was acquired.

10 To evoke MF synaptic responses in MCs and CA3 pyramidal cells, a bipolar stimulating theta-
11 glass pipette was filled with ACSF and placed in the subgranular zone of the DG. Only EPSCs
12 that showed < 2 ms 20-80% rise time and robust paired-pulse facilitation (EPSC2/EPSC1 > 2)
13 were considered MF-derived and included in the analysis.

14 To increase the probability of detecting a KAR-mediated EPSC, we delivered two stimuli (5 ms
15 inter-stimulus interval, 100 μ s duration, ~100 μ A amplitude), using a stimulus isolator unit (Isoflex,
16 AMPI). Typically, stimulation was adjusted to obtain comparable magnitude synaptic responses
17 across experiments.

18

19 **Data analysis for electrophysiology experiments**

20 Electrophysiological data were acquired at 5 kHz filtered at 2.4 kHz and analyzed using custom-
21 made software for IgorPro (Wavemetrics Inc.). The change in the holding current (ΔI holding) was
22 calculated by subtracting the baseline holding current value (average of 50 s before KA
23 application) from the average holding current post-drug application (average 50 s before
24 washout). To calculate firing rate in the current clamp configuration, spikes were detected using
25 a custom-made MatLab script, which detected all voltage increases above a threshold value
26 established by the experimenter (i.e., 0 mV). When 3 μ M KA was used to depolarize MCs, the
27 peak of the action potentials gradually decreased (likely due to inactivation of voltage-gated
28 sodium channels) and became undistinguishable from spontaneous activity. This led to an
29 underestimation of the effect of 3 μ M KA on MCs firing. Firing rate was quantified as number of
30 spikes per second.

31

1 **Reagents**

2 Reagents were bath applied following dilution into ACSF from stock solutions stored at -20°C
3 prepared in water or DMSO, depending on the manufacturer's recommendation. The final DMSO
4 concentration was <0.01% total volume. All chemicals and drugs used for the electrophysiology
5 experiments were purchased from Sigma-Aldrich (St. Louis, MO, USA) except NBQX, CGP-
6 55845, DCG-IV, and GYKI 53655, which were obtained from Tocris-Cookson (Minneapolis, MN,
7 USA), and tetrodotoxin, which was obtained from HelloBio (Inc, Princeton, NJ). LY 303070 was
8 obtained from ABX advanced biochemical compounds (Radeberg, Germany).

9

10 **Quantification and statistical analysis.**

11 Statistical analysis was performed using OriginPro software (OriginLab). The normality of
12 distributions was assessed using the Shapiro-Wilk test. In normal distributions, Student's unpaired
13 and paired t Tests were used to assess between-group and within-group differences, respectively.
14 The non-parametric paired sample Wilcoxon signed rank test and Mann-Whitney's U test were
15 used in non-normal distributions. Statistical significance was set to $p < 0.05$ (***) indicates $p <$
16 0.001 , ** indications $p < 0.01$, and * indicates $p < 0.05$). All values are reported as the mean \pm
17 SEM.

18

19 **Fixation and sections**

20 We used glyoxal fixative containing 9% glyoxal and 8% acetic acid (v/v, pH 4.0 adjusted with 5N
21 NaOH), which is modified from the original glyoxal fixative (Richter et al., 2018). Under deep
22 pentobarbital anesthesia (100 mg/kg body weight, i.p.), mice were fixed by transcardial perfusion
23 with ~60 ml of glyoxal solution for 10 min at room temperature. Brains were postfixed in the same
24 fixative for 3 h and cryoprotected with 30% sucrose in 0.1 M PB (pH 7.2) for 2 d. For
25 immunofluorescence and immunoelectron microscopy, 50- μ m-thick coronal sections through the
26 ventral hippocampus (3.0–3.7 mm posterior to Bregma) were prepared on a cryostat (CM1900;
27 Leica Microsystems) and subjected to free-floating incubation.

28

29 **Antibodies**

30 We used the following antibodies: mouse anti-calretinin (MAB1568, Millipore; RRID, AB_94259),
31 goat anti-EGFP (Takasaki et al., 2010)(AB_2571574), rabbit anti-GluK2/3 (Straub et al., 2011),

1 guinea pig anti-Neto1 (Straub et al., 2011), and guinea pig anti-PSD95 (Fukaya and Watanabe,
2 2000)(AB_2571612).

3

4 **Immunofluorescence**

5 All immunohistochemical procedures for immunofluorescence were performed at room
6 temperature and PBS containing 0.1% Triton-X100 was used as a dilution and washing buffer.
7 Sections were incubated with 10% normal donkey serum for 20 min, a mixture of primary
8 antibodies overnight (1 µg/ml each), and a mixture of Alexa Fluor 405-, 488-, 647-, or Cy3-labeled
9 species-specific secondary antibodies for 2 h at a dilution of 1:200 (Invitrogen; Jackson
10 ImmunoResearch). To avoid cross talk between multiple fluorophores, images were taken with a
11 confocal laser-scanning microscope equipped with 405-, 473-, 559-, and 647-nm diode laser
12 lines, and UPLSAPO 10× (NA, 0.4), and PLAPON 60×OSC2 (NA, 1.4; oil immersion) objective
13 lenses (FV1200, Olympus). Image and pinhole size were 800 × 800 pixels and 1 airy unit,
14 respectively. To compare genotypic and regional difference, images were taken at the same
15 condition.

16

17 **Preembedding immunoelectron microscopy**

18 All incubations were performed at room temperature and PBS containing 0.1% Tween20 was
19 used as a dilution and washing buffer. Sections were incubated in 10% normal goat serum
20 (Nichirei, Tokyo, Japan) for 20 min, and with primary antibody against GluK2/3 (1 µg/ml) overnight
21 and then with secondary antibodies linked to 1.4-nm gold particles (1:100; Nanogold;
22 Nanoprobes) for 4 h. After extensive washing with PBST and HEPES buffer (200 mM sucrose,
23 50 mM HEPES, pH 8.0), immunogold was intensified with a silver enhancement kit (R-GENT SE-
24 EM; Aurion) for 45–60 min. Sections were further treated with 1% osmium tetroxide for 15 min,
25 stained with 2% uranyl acetate for 20 min, dehydrated with graded ethanol series, and embedded
26 in Epon 812 (TAAB). After polymerization at 60°C for 48 h, ultrathin sections were prepared with
27 an ultramicrotome (Ultracut; Leica), mounted on copper-mesh grids and stained with 2% uranyl
28 acetate for 5 min and Reynold's lead citrate solution for 1 min. Photographs were taken with a
29 JEM1400 electron microscope (JEOL, Tokyo, Japan). Electron micrographs were randomly taken
30 within ~5 µm from the surface to avoid false-negative areas. To quantify metal particle labeling, 3
31 × 3 montage images (~6 µm × 6 µm) were randomly taken at a magnification of 15,000×.

1 For quantitative analysis, plasma membrane-attached immunogold particles, being defined as
2 those apart <35 nm from the cell membrane, were counted and analyzed using MetaMorph
3 software (Molecular Devices). The mean number of membrane-attached gold particles per 1 μm
4 of the plasma membrane was counted for each neuronal compartment (dendritic spine, dendritic
5 shaft, and soma). Measurements were made from three WT and two *Gluk2* KO mice and pooled
6 together, because there was no significant difference in the labeling density in the same genotype.
7 In each neuronal compartment, labeling density was calculated for individual profile. Statistical
8 analyses were performed using GraphPad Prism 9.0 software (GraphPad Software). All data are
9 given as mean \pm SEM. Data were analyzed using Kruskal-Wallis test followed by Dunn's post
10 Test. * $p < 0.05$; ** $p < 0.01$; *** $p < 0.001$.

11

12 **Results**

13

14 **Kainate receptors mediate inward currents and action potential firing in hilar mossy cells**

15 To test whether MCs expressed functional KARs, we first performed whole-cell patch clamp
16 recordings from MCs in acute rat hippocampal slices and bath applied the KAR agonist KA. MCs
17 were identified based on the high frequency of spontaneous EPSCs, non-burst firing pattern upon
18 depolarization, and action potentials with almost no afterhyperpolarization (see Methods) (Larimer
19 and Strowbridge, 2008) (**Fig. 1A**). To confirm the identity of the recorded cell, we loaded putative
20 MCs with biocytin and stained with Alexa 594-conjugated streptavidin, and confirmed the
21 presence of TEs, a hallmark of MCs (**Fig. 1A**) (Scharfman and Schwartzkroin, 1988). We
22 examined whether KA bath application induced KAR-mediated inward currents in MCs, as
23 previously shown in KAR-expressing CA3 pyramidal cells (Castillo et al., 1997; Mulle et al., 1998)
24 To isolate these currents, recordings were performed in the presence of LY303070 (15 μM), D-
25 APV (25 μM), picrotoxin (50 μM) and CGP35348 (3 μM) to block AMPARs, NMDARs, GABA_A and
26 GABA_B receptors, respectively, and MCs were voltage clamped at -60 mV. Under these recording
27 conditions, KA bath application (0.3 μM and 3 μM) induced large, concentration-dependent inward
28 currents in MCs (**Fig. 1B,C**) (ΔI holding MC: 0.3 μM KA: 165.3 ± 28.56 pA; $n = 5a/5c$; 3 μM KA:
29 736.24 ± 82.34 pA; $n = 4a/4c$ – one of the cells died after 0.3 μM application). In contrast, the
30 same concentrations of KA induced modest currents in GCs (ΔI holding GC: 0.3 μM KA: $30.73 \pm$
31 1.38 pA; $n = 3a/3c$; 3 μM KA: 72.21 ± 6.31 pA; $n = 3a/3c$). By activating KARs in CA3 pyramidal
32 cells, KA application could recruit CA3 pyramidal cells (Robinson and Deadwyler, 1981;

1 Westbrook and Lothman, 1983; Castillo et al., 1997) which make synaptic contacts with MCs
2 (Scharfman, 1994) and could indirectly activate KARs in MCs. To test this possibility, action
3 potential generation was prevented by perfusing the voltage-gated sodium channel blocker
4 tetrodotoxin (TTX, 0.5 μ M) in the bath. In the presence of TTX, KA-induced currents were not
5 significantly different from control conditions (**Fig. 1D,E**) (Δ I holding MC + TTX, 0.3 μ M KA : 117.3
6 \pm pA; n = 5a/6c; 3 μ M KA: 765.19 \pm 79.06 pA; n = 5a/6c; 0.3 μ M control vs TTX: n.s. p = 0.12045,
7 two sample t Test; 3 μ M control vs TTX: n.s. p = 0.81287: two sample t Test), indicating that these
8 currents do not result from indirect activation of CA3 pyramidal neurons. In addition, the
9 competitive AMPAR/KAR antagonist NBQX (25 μ M) abolished KA-mediated inward currents,
10 strongly suggesting these currents were mediated by KAR activation in MCs (**Fig. 1D,E**) (Δ I
11 holding MC 0.3 μ M KA control: 182.78 \pm 25.7 pA; n = 3a/4c; 3 μ M KA + 25 μ M NBQX: 12.99 \pm
12 3.31; n = 3a/4c; 0.3 μ M KA vs 3 μ M KA + NBQX: *** p = 0.000012: two sample t Test). Lastly, KA
13 bath application induced currents in MCs of mouse hippocampal slices, which were abolished in
14 *Gluk2* KO mice (**Fig. 1F,G**) (Δ I holding MC WT; 0.1 μ M KA: 58.33 \pm 19.49 pA, 0.3 μ M KA: 75.44
15 \pm 13.87, 1 μ M KA: 233.91 \pm 15.67 pA, 3 μ M KA: 494.32 \pm 85.01 pA; Δ I holding *Gluk2* KO; 0.1 μ M
16 KA: 19.77 \pm 9.27 pA, 0.3 μ M KA: 13.35 \pm 4.44 pA, 1 μ M KA: 24.74 \pm 10.55 pA, 3 μ M KA: 14.39 \pm
17 5.04 pA; WT vs *Gluk2* KO: $F(1,3) = 146.98864$, ** p = 0.00121; two-way ANOVA repeated
18 measures), indicating that these currents are mediated by GluK2-containing KARs.

19

20 We hypothesized that KAR-mediated currents can produce enough depolarization to drive MC
21 action potential firing. To test this possibility, we recorded MCs in current-clamp mode before and
22 after KA application. Given that hippocampal interneurons impinging on MCs could express
23 functional KARs (Frerking et al., 1998), these experiments were performed with intact excitatory
24 and inhibitory components of synaptic transmission in order to assess the net effect of KAR
25 activation on MC firing. Under these recording conditions, bath application of 0.3 μ M and 3.0 μ M
26 KA induced strong MC firing (**Fig. 2A**) (WT average firing rate 0.3 μ M KA: 0.333 μ M \pm 0.025
27 spikes/s; n = 2a/3c; 3 μ M KA: 5.54 \pm 0.28; n = 2a/3c), and this effect was abolished in *Gluk2* KO
28 mice (**Fig. 2B**). These results indicate that activation of GluK2-containing KARs with low
29 concentrations of the agonist KA can powerfully drive MCs.

30

31 **KARs-mediated EPSCs are undetectable at MF-MC synapse**

1 We next sought to determine the subcellular localization of KARs on MCs. Because of the strong
2 structural and functional similarities between CA3 pyramidal cells and MCs, we tested whether
3 MF activation elicits KAR-EPSCs in MCs as previously shown at MF inputs onto CA3 pyramidal
4 cells (Castillo et al., 1997). To this end, we evoked AMPAR-EPSCs by stimulating MF axons with
5 two stimuli to boost glutamate release from MFs (5 ms inter-stimulus interval) in the presence of
6 a cocktail of NMDARs, GABA_A and GABA_B receptor antagonists (see Methods). We then
7 attempted to isolate the KAR-mediated component of the MF-EPSC by applying the selective,
8 non-competitive AMPAR antagonist GYKI 53655 (30 μM). GYKI application abolished the
9 AMPAR-EPSCs but surprisingly, it failed to uncover a KAR-mediated EPSC (**Fig. 3A**) (EPSC
10 amplitude post GYKI application: 2.35 ± 0.52 % of baseline; n = 4a/5s). In addition, increasing the
11 number of stimuli (from 2 to 5), a manipulation expected to increase the likelihood of detecting
12 KAR-EPSCs at the MF-CA3 synapse (Castillo et al., 1997), did not generate any detectable
13 current either (data not shown; 5 pulses: 2.108 ± 0.415 % of baseline; n = 4a/5s). To verify that
14 the EPSCs were MF-mediated, in a separate set of experiments, we applied the mGluR2/3
15 agonist DCG-IV (1 μM) which selectively blocks glutamate release at MF-MC synapses (**Fig. 3B**)
16 (Lysetskiy et al., 2005; Hedrick et al., 2017). DCG-IV reduced synaptic responses by ~70 %,
17 indicating our stimulation mainly recruited MF inputs onto MCs (EPSC amplitude post DCG IV:
18 29.35 ± 7.07 % of baseline; n = 3a/4s). As a positive control, and as previously reported (Castillo
19 et al., 1997), MF stimulation elicited GYKI-resistant, NBQX-sensitive KAR-EPSCs in CA3
20 pyramidal neurons (**Fig. 3C**) (EPSC amplitude post GYKI application: 15.85 ± 6.59 % of baseline;
21 n = 2a/4s; KAR-EPSC amplitude post NBQX application: 0.47 ± 0.25 % of baseline; n = 2a/4s).
22 These results indicate that in contrast to MF-CA3 synapses, KARs do not mediate synaptic
23 transmission at MF-MC synapses. Given the robust activation of MCs by low concentrations of
24 KA (Figs. 1,2), our findings thus far suggest KARs in MCs are extrasynaptic.

25

26 **Distinct subcellular localization of KARs in CA3 pyramidal cells and mossy cells**

27 To determine the anatomical localization of KARs in MCs, we applied immunostaining to tissue
28 sections fixed with a glyoxal-based fixative (see Methods), which is effective for detection of both
29 non-synaptic and synaptic molecules. First, we confirmed the specificity of the antibody against
30 GluK2/3 by blank labeling in *GluK2* KO hippocampus (**Fig. 4A,B**). In WT mice, the antibody
31 yielded a contrasting pattern of labeling across hippocampal subregions: intense and coarse
32 punctate labeling in the CA3 *stratum lucidum*, and moderate and diffuse labeling in the hilus (**Fig**
33 **4A**). Further quadplex immunofluorescence using *GAD67*^{+GFP} mice (Tamamaki et al., 2003)

1 allowed us to distinguish excitatory MCs from inhibitory calretinin-positive interneurons, and to
2 examine if MCs express GluK2/3 (**Fig. 4C,D**) together with or without the excitatory postsynaptic
3 marker PSD95 (**Fig. 4C**), or the KAR auxiliary subunit Neto1 (**Fig. 4D**). In CA3 *stratum lucidum*,
4 GluK2/3-positive puncta were intense and aggregated into large clusters and were almost
5 perfectly overlapped with PSD95 (**Fig. 4E,F**), suggesting exclusive localization in MF-CA3
6 pyramidal cell synapse. Compared with CA3, GluK2/3 labeling was smaller and less frequent in
7 the hilus of the DG (**Fig. 4G,H**). MC soma and dendrites, which can be unequivocally identified
8 as calretinin-positive and GFP-negative structures (**Fig. 4G**), were associated with GluK2/3
9 puncta that did not colocalize with PSD95 (**Fig. 4H**). Similarly, while Neto1 staining was
10 overlapped with GluK2/3-positive puncta in *stratum lucidum* (**Fig. 4I,J**), it was not found around
11 MC soma and dendrites (**Fig. 4K,L**). Together, these findings suggest that GluK2/3-containing
12 KARs in MCs are expressed at extrasynaptic sites.

13 For a more accurate assessment of the subcellular localization of KARs in MCs, we performed
14 pre-embedding immunoelectron microscopy for GluK2/3. In WT mice, metal particles for GluK2/3
15 were observed on the postsynaptic membrane of TEs (**Fig. 5A,G**, blue) of CA3 pyramidal cells
16 facing large MF boutons (12.1 ± 0.95 particles/mm). In *GluK2* KO mice, immunolabeling was
17 essentially absent on the postsynaptic membrane of CA3 spines (**Fig. 5B,G** blue), confirming the
18 specificity of the immunolabeling (0.07 ± 0.07 particles/mm; Dunn's multiple comparison test; $p <$
19 0.0001 , compared to WT). In the DG hilus, MCs can be identified as having spiny dendrites
20 contacted with large MF terminals (Acsady et al., 1998). In contrast to MF-CA3 synapses, MF-
21 MC synapses were not labeled for GluK2/3 (**Fig. 5C,G**) (0.06 ± 0.04 particles/ μm in WT, vs 0.01
22 ± 0.01 particles/ μm in *GluK2* KO; $p > 0.99$). Instead, occasional weak labeling was observed on
23 the non-synaptic membrane of dendritic shaft and spines of MCs (**Fig. 5E,F** green). The density
24 of non-synaptic particles was much lower than that at MF-CA3 synapses ($p = 0.0137$), but
25 significantly higher than their counterparts in *GluK2* KO (**Fig. 5D,G**; 4.1 ± 0.8 particles/ μm in WT
26 vs 0.02 ± 0.01 particles/ μm in *GluK2* KO; $p = 0.008$). These results not only demonstrate the
27 presence of KARs in MCs but also show that, in contrast to CA3 pyramidal neurons, GluK2-
28 containing KARs are exclusively expressed at non-synaptic sites in proximity of MF-MC synapses.

29

30 **Activation of KARs in mossy cells by increase in ambient glutamate.**

31 Given the extracellular location of KARs in MCs we hypothesized that these receptors are
32 activated by ambient glutamate. To test this possibility, we blocked excitatory amino acid

1 transporters (EAATs), a manipulation that can raise extracellular glutamate and activate
2 extrasynaptic NMDARs (Le Meur et al., 2007). We first examined the effect of the non-selective
3 EAAT blocker DL-TBOA (100 μ M) on MC holding current in presence of antagonists of AMPARs,
4 NMDAR, GABA_A and GABA_B receptors (see Methods). Bath application of TBOA mediated a
5 significant NBQX-sensitive inward current in MCs, suggesting that KARs could be activated by
6 endogenous glutamate (**Fig 6A-C**) (Δ I holding MC + TBOA: 61.24 ± 18.61 pA; * $p = 0.02173$ one
7 sample t Test). We next used the more selective blocker dihydrokainic acid (DHK), which
8 selectively blocks EAAT2 (GLT-1), a glutamate transporter that accounts for ~90% of glutamate
9 uptake (Rose et al., 2017) and is enriched in the telencephalon including the hippocampus
10 (Chaudhry et al., 1995). Bath application of 100 μ M DHK also induced NBQX-sensitive inward
11 currents in MCs (**Fig. 6A-C**), strongly suggesting that DHK-induced currents are mediated by
12 activation of KARs (Δ I holding MC + DHK: 28.06 ± 7.4 pA; $n = 3a/6c$; $n = 4a/6c$). To determine
13 that DHK-induced currents was due to activation of KARs, we repeated the experiment in *GluK2*
14 KO mice, and found that in these mice DHK failed to induce inward currents in MCs (**Fig. 6A,C**)
15 (Δ I holding MC + DHK *GluK2* KO: -8.5 ± 7.47 ; $n = 3a/4c$; DHK vs DHK *GluK2* KO mice: * $p =$
16 0.0105 two sample t Test). These finding suggest that increases in ambient glutamate can
17 activate extrasynaptic MC-KARs.

18

19 **DISCUSSION**

20

21 In this study, we provide functional and anatomical evidence that MCs express extrasynaptic
22 KARs whose activation in the rodent hippocampus can drive MCs. Specifically, we show that low
23 concentrations of KA induced inward currents and action potential firing of MCs. In contrast, KA-
24 induced currents were nearly absent in GCs, indicating that KARs have a unique pattern of
25 expression among excitatory cells in the DG. Unexpectedly, MF activation failed to evoke a KAR-
26 EPSCs in MCs, indicating that MF-MC synapses, unlike MF-CA3 synapses, do not normally
27 express synaptic KARs. Our immunofluorescence and immunoelectron microscopy data
28 confirmed that KARs in MCs are sparsely distributed at extrasynaptic sites and mainly excluded
29 from postsynaptic compartments. Finally, blockade of the astrocytic glutamate transporter EAAT2
30 revealed that MC-KARs can be activated by increasing ambient glutamate.

31

1 The presence of extrasynaptic KARs has previously been suggested in hippocampal CA1
2 pyramidal neurons (Bureau et al., 1999), striatal medium spiny neurons (Chergui et al., 2000) and
3 cortical layer V pyramidal neurons (Eder et al., 2003). These functional studies inferred the
4 presence of extrasynaptic KARs given the robust effects to bath applied KAR agonist (e.g.,
5 membrane depolarization, inward current, action potential firing) with little evidence for KAR-
6 mediated EPSCs. Of note, none of these studies provided ultrastructural evidence in support of
7 extrasynaptic KARs. To the best of our knowledge, our immunoelectron microscopy data together
8 with our electrophysiological characterization is the first direct evidence of a selective
9 extrasynaptic localization of functional KARs in the mammalian brain.

10

11 Given the similarities between MF-CA3 and MF-MC synapses, the absence of KARs at MF-MC
12 synapses is intriguing. Based on the presence of a GYKI-resistant component following MF
13 stimulation, a previous study reported the presence of postsynaptic KARs in MCs (Hedrick et al.,
14 2017). However, these currents were not validated in *GluK2* KO mice and showed relatively fast
15 kinetics, which is unusual for KAR-EPSCs. Our study does not discard the possibility that KARs
16 could be expressed at MF-MC synapses early during development (Lauri and Taira, 2011; Lerma
17 and Marques, 2013). The molecular mechanisms that target KARs to the synapse remain unclear,
18 but several KAR interacting proteins such as Neto 1 and 2 (Straub et al., 2011; Tomita and
19 Castillo, 2012; Wyeth et al., 2014), N-cadherins (Coussen et al., 2002; Fievre et al., 2016) and
20 presynaptic C1ql family proteins (Matsuda et al., 2016; Straub et al., 2016) may contribute.
21 Consistent with data derived from a population-level transcriptomics study in the hippocampus
22 (Cembrowski et al., 2016), we found that Neto1 signal was absent from MCs (Fig. 4), suggesting
23 that lack of Neto1 could contribute to the low expression of KARs at the synapse (Wyeth et al.,
24 2014). However, lack of GluK2-containing KARs also leads to reduced levels of Neto1 (Straub et
25 al., 2011). The C-terminal domain of KARs themselves is important for the synaptic stabilization
26 of KARs in the cerebellum (Straub et al., 2016). Additionally, phosphorylation of specific residues
27 in the C-terminal and other intracellular regions of KARs has been implicated in the modulation of
28 KARs function and trafficking (Wang et al., 1993; Kornreich et al., 2007; Carta et al., 2013; Zhu
29 et al., 2014). Further studies are required to clarify the molecular mechanisms that determine the
30 exclusion of KARs from MF-MC synapses.

31

1 Like other extrasynaptic receptors, KARs in MCs could be engaged by a rise in ambient
2 glutamate, which can occur as a result of glutamate spillover during sustained synaptic activity
3 (Le Meur et al., 2007; Rose et al., 2017). Glutamate could also arise from MC dendrites, as
4 previously reported in neocortical and cerebellar neurons (Zilberter, 2000; Shin et al., 2008), and
5 activate extrasynaptic KARs. We found that blockade of EAAT2 induces KAR-mediated inward
6 currents likely due to the increase in extracellular glutamate. In the CA1 area of the hippocampus,
7 activation of extrasynaptic receptors by synaptically released glutamate is limited by efficient
8 astrocytic EAAT2 activity (Diamond and Jahr, 2000), consistent with a neuroprotective role of this
9 transporter (Kong et al., 2012; Pajarillo et al., 2019). However, EAAT2 may saturate in other brain
10 areas (Armbruster et al., 2016; Pinky et al., 2018). EAAT2 saturation during neuronal hyperactivity
11 could enable the activation of extrasynaptic KARs at MCs. Alternatively, extrasynaptic KARs could
12 be activated by glutamate released from astrocytes (Araque et al., 2014; Pal, 2015), as previously
13 reported in CA1 GABAergic interneurons (Liu et al., 2004). There is evidence that glutamate
14 released from astrocytes can also activate extrasynaptic NMDARs in CA1 pyramidal neurons
15 (Fellin et al., 2004), and depolarize both hilar GABAergic interneurons and MCs (Pabst et al.,
16 2016). These depolarizations were blocked by non-selective antagonism of all ionotropic
17 glutamate receptors, raising the possibility that extrasynaptic KARs could be implicated. Future
18 work is required to determine whether astrocytic processes (Gavrilov et al., 2018) could release
19 glutamate in proximity to extrasynaptic KARs, thereby avoiding glutamate uptake by EAAT2.

20

21 Although the precise role for extrasynaptic KARs in MCs is unclear, they might detect changes in
22 the levels of ambient glutamate and mediate tonic depolarization. *In vivo*, MCs display high level
23 of activity compared to neighboring GCs (Danielson et al., 2017; GoodSmith et al., 2017; Senzai
24 and Buzsaki, 2017). In standard home cage rats, MCs stain positive for the activity-dependent
25 immediately early gene *cFos* (Duffy et al., 2013), suggesting that even at the basal level, MCs are
26 remarkably active. It is possible that in behaving animals, where spontaneous activity is most
27 likely higher than *in vitro*, glutamate might escape reuptake by EAATs and activate extrasynaptic
28 KARs. During periods of particularly high activity and potential EAAT2 saturation, KARs might act
29 as nonlinear integrators of synaptic inputs, and enhance MC output. KARs can also work in a
30 metabotropic fashion and could potentially affect MCs excitability by suppressing the slow
31 afterhyperpolarization (Melyan et al., 2002; Ruiz et al., 2005). Ultimately, MC-KARs could
32 contribute to the promiscuous activity of MCs in multiple locations and environments (Danielson
33 et al., 2017; GoodSmith et al., 2017; Senzai and Buzsaki, 2017).

1

2 Both MCs and KARs have been linked to several neurological and psychiatric disorders (Ratzliff
3 et al., 2002; Lerma and Marques, 2013; Scharfman, 2016). Of particular relevance is the strong
4 link between KARs and MCs with TLE. KARs have been strongly implicated in epilepsy (Crepel
5 and Mulle, 2015; Falcon-Moya et al., 2018), and KA-induced TLE is one of the most widely used
6 models of TLE (Levesque and Avoli, 2013; Rusina et al., 2021). The importance of KARs in KA-
7 induced TLE is highlighted by the fact that loss of GluK2-containing KARs, strongly reduces the
8 susceptibility to KA-induced seizures (Mulle et al., 1998). Similarly, MCs have been proposed to
9 have a proepileptogenic role in the early phases of TLE (Ratzliff et al., 2002; Botterill et al., 2019)
10 and to undergo prominent cell-death in both animal models of epilepsy (Blumcke et al., 2000) and
11 in human patients (Margerison and Corsellis, 1966; Seress et al., 2009). However, the precise
12 mechanism through which KARs and MCs are involved in TLE is still unclear. Expression of KARs
13 in MCs strongly suggests that MCs could be a direct target of KA in KA-induced TLE. KA-induced
14 MCs firing could contribute to hyperexcitability of the associative GC-MC-GC network and to the
15 generation of seizures. Moreover, sustained KAR-mediated MCs firing could be a critical trigger
16 for long-lasting forms of plasticity in the DG associative network (Hashimoto et al., 2017),
17 which could contribute to the prolongation of epileptic activity. A major limitation for the study of
18 MC function in behavior is the lack of molecular tools that target MCs specifically. Thus far,
19 manipulation of MCs activity *in vivo* relied on viral delivery of constructs under the control of
20 promoters that are not highly specific for MCs (Jinde et al., 2012; Puighermanal et al., 2015).
21 Establishing the precise role of MC-KARs on hippocampal function and TLE will require novel
22 strategies such as intersectional genetics approaches (Dymecki et al., 2010; Graybuck et al.,
23 2021) that will allow more selective targeting of MCs while sparing neighboring KAR-expressing
24 cells such as CA3 pyramidal neurons and hilar interneurons.

25

26

27

1

References

- 2 Acsady L, Kamondi A, Sik A, Freund T, Buzsaki G (1998) GABAergic cells are the major postsynaptic targets
3 of mossy fibers in the rat hippocampus. *J Neurosci* 18:3386-3403.
- 4 Amaral DG, Dent JA (1981) Development of the mossy fibers of the dentate gyrus: I. A light and electron
5 microscopic study of the mossy fibers and their expansions. *J Comp Neurol* 195:51-86.
- 6 Araque A, Carmignoto G, Haydon PG, Oliet SH, Robitaille R, Volterra A (2014) Gliotransmitters travel in
7 time and space. *Neuron* 81:728-739.
- 8 Armbruster M, Hanson E, Dulla CG (2016) Glutamate Clearance Is Locally Modulated by Presynaptic
9 Neuronal Activity in the Cerebral Cortex. *J Neurosci* 36:10404-10415.
- 10 Blumcke I, Suter B, Behle K, Kuhn R, Schramm J, Elger CE, Wiestler OD (2000) Loss of hilar mossy cells in
11 Ammon's horn sclerosis. *Epilepsia* 41 Suppl 6:S174-180.
- 12 Botterill JJ, Lu YL, LaFrancois JJ, Bernstein HL, Alcantara-Gonzalez D, Jain S, Leary P, Scharfman HE (2019)
13 An Excitatory and Epileptogenic Effect of Dentate Gyrus Mossy Cells in a Mouse Model of Epilepsy.
14 *Cell Rep* 29:2875-2889 e2876.
- 15 Buckmaster PS, Schwartzkroin PA (1994) Hippocampal mossy cell function: a speculative view.
16 *Hippocampus* 4:393-402.
- 17 Buckmaster PS, Jongen-Relo AL (1999) Highly specific neuron loss preserves lateral inhibitory circuits in
18 the dentate gyrus of kainate-induced epileptic rats. *J Neurosci* 19:9519-9529.
- 19 Buckmaster PS, Wenzel HJ, Kunkel DD, Schwartzkroin PA (1996) Axon arbors and synaptic connections of
20 hippocampal mossy cells in the rat in vivo. *J Comp Neurol* 366:271-292.
- 21 Bureau I, Bischoff S, Heinemann SF, Mulle C (1999) Kainate receptor-mediated responses in the CA1 field
22 of wild-type and GluR6-deficient mice. *J Neurosci* 19:653-663.
- 23 Carta M, Opazo P, Veran J, Athane A, Choquet D, Coussen F, Mulle C (2013) CaMKII-dependent
24 phosphorylation of GluK5 mediates plasticity of kainate receptors. *EMBO J* 32:496-510.
- 25 Castillo PE, Malenka RC, Nicoll RA (1997) Kainate receptors mediate a slow postsynaptic current in
26 hippocampal CA3 neurons. *Nature* 388:182-186.
- 27 Cembrowski MS, Wang L, Sugino K, Shields BC, Spruston N (2016) HippoSeq: a comprehensive RNA-seq
28 database of gene expression in hippocampal principal neurons. *Elife* 5:e14997.
- 29 Chaudhry FA, Lehre KP, van Lookeren Campagne M, Ottersen OP, Danbolt NC, Storm-Mathisen J (1995)
30 Glutamate transporters in glial plasma membranes: highly differentiated localizations revealed by
31 quantitative ultrastructural immunocytochemistry. *Neuron* 15:711-720.
- 32 Chergui K, Bouron A, Normand E, Mulle C (2000) Functional GluR6 kainate receptors in the striatum:
33 indirect downregulation of synaptic transmission. *J Neurosci* 20:2175-2182.
- 34 Coussen F, Normand E, Marchal C, Costet P, Choquet D, Lambert M, Mege RM, Mulle C (2002) Recruitment
35 of the kainate receptor subunit glutamate receptor 6 by cadherin/catenin complexes. *J Neurosci*
36 22:6426-6436.
- 37 Crepel V, Mulle C (2015) Physiopathology of kainate receptors in epilepsy. *Curr Opin Pharmacol* 20:83-88.
- 38 Danielson NB, Turi GF, Ladow M, Chavlis S, Petrantonakis PC, Poirazi P, Losonczy A (2017) In Vivo Imaging
39 of Dentate Gyrus Mossy Cells in Behaving Mice. *Neuron* 93:552-559 e554.
- 40 Diamond JS, Jahr CE (2000) Synaptically released glutamate does not overwhelm transporters on
41 hippocampal astrocytes during high-frequency stimulation. *J Neurophysiol* 83:2835-2843.
- 42 Duffy AM, Schaner MJ, Chin J, Scharfman HE (2013) Expression of c-fos in hilar mossy cells of the dentate
43 gyrus in vivo. *Hippocampus* 23:649-655.
- 44 Dymecki SM, Ray RS, Kim JC (2010) Mapping cell fate and function using recombinase-based intersectional
45 strategies. *Methods Enzymol* 477:183-213.

- 1 Eder M, Becker K, Rammes G, Schierloh A, Azad SC, Zieglgansberger W, Dodt HU (2003) Distribution and
2 properties of functional postsynaptic kainate receptors on neocortical layer V pyramidal neurons.
3 *J Neurosci* 23:6660-6670.
- 4 Falcon-Moya R, Sihra TS, Rodriguez-Moreno A (2018) Kainate Receptors: Role in Epilepsy. *Front Mol*
5 *Neurosci* 11:217.
- 6 Fellin T, Pascual O, Gobbo S, Pozzan T, Haydon PG, Carmignoto G (2004) Neuronal synchrony mediated by
7 astrocytic glutamate through activation of extrasynaptic NMDA receptors. *Neuron* 43:729-743.
- 8 Fievre S, Carta M, Chamma I, Labrousse V, Thoumine O, Mulle C (2016) Molecular determinants for the
9 strictly compartmentalized expression of kainate receptors in CA3 pyramidal cells. *Nat Commun*
10 7:12738.
- 11 Fredes F, Silva MA, Koppensteiner P, Kobayashi K, Joesch M, Shigemoto R (2021) Ventro-dorsal
12 Hippocampal Pathway Gates Novelty-Induced Contextual Memory Formation. *Curr Biol* 31:25-38
13 e25.
- 14 Frerking M, Malenka RC, Nicoll RA (1998) Synaptic activation of kainate receptors on hippocampal
15 interneurons. *Nat Neurosci* 1:479-486.
- 16 Frotscher M, Seress L, Schwerdtfeger WK, Buhl E (1991) The mossy cells of the fascia dentata: a
17 comparative study of their fine structure and synaptic connections in rodents and primates. *J*
18 *Comp Neurol* 312:145-163.
- 19 Fukaya M, Watanabe M (2000) Improved immunohistochemical detection of postsynaptically located
20 PSD-95/SAP90 protein family by protease section pretreatment: a study in the adult mouse brain.
21 *J Comp Neurol* 426:572-586.
- 22 Gavrilov N, Golyagina I, Brazhe A, Scimemi A, Turlapov V, Semyanov A (2018) Astrocytic Coverage of
23 Dendritic Spines, Dendritic Shafts, and Axonal Boutons in Hippocampal Neuropil. *Front Cell*
24 *Neurosci* 12:248.
- 25 GoodSmith D, Chen X, Wang C, Kim SH, Song H, Burgalossi A, Christian KM, Knierim JJ (2017) Spatial
26 Representations of Granule Cells and Mossy Cells of the Dentate Gyrus. *Neuron* 93:677-690 e675.
- 27 Graybuck LT et al. (2021) Enhancer viruses for combinatorial cell-subclass-specific labeling. *Neuron*.
- 28 Hashimoto-dani Y, Nasrallah K, Jensen KR, Chavez AE, Carrera D, Castillo PE (2017) LTP at Hilar Mossy Cell-
29 Dentate Granule Cell Synapses Modulates Dentate Gyrus Output by Increasing
30 Excitation/Inhibition Balance. *Neuron* 95:928-943 e923.
- 31 Hedrick TP, Nobis WP, Foote KM, Ishii T, Chetkovich DM, Swanson GT (2017) Excitatory Synaptic Input to
32 Hilar Mossy Cells under Basal and Hyperexcitable Conditions. *eNeuro* 4.
- 33 Henze DA, Wittner L, Buzsaki G (2002) Single granule cells reliably discharge targets in the hippocampal
34 CA3 network in vivo. *Nat Neurosci* 5:790-795.
- 35 Jinde S, Zsiros V, Jiang Z, Nakao K, Pickel J, Kohno K, Belforte JE, Nakazawa K (2012) Hilar mossy cell
36 degeneration causes transient dentate granule cell hyperexcitability and impaired pattern
37 separation. *Neuron* 76:1189-1200.
- 38 Kamiya H, Shinozaki H, Yamamoto C (1996) Activation of metabotropic glutamate receptor type 2/3
39 suppresses transmission at rat hippocampal mossy fibre synapses. *J Physiol* 493 (Pt 2):447-455.
- 40 Kong Q, Takahashi K, Schulte D, Stouffer N, Lin Y, Lin CL (2012) Increased glial glutamate transporter EAAT2
41 expression reduces epileptogenic processes following pilocarpine-induced status epilepticus.
42 *Neurobiol Dis* 47:145-154.
- 43 Kornreich BG, Niu L, Roberson MS, Oswald RE (2007) Identification of C-terminal domain residues involved
44 in protein kinase A-mediated potentiation of kainate receptor subtype 6. *Neuroscience* 146:1158-
45 1168.
- 46 Larimer P, Strowbridge BW (2008) Nonrandom local circuits in the dentate gyrus. *J Neurosci* 28:12212-
47 12223.

- 1 Lauri SE, Taira T (2011) Role of kainate receptors in network activity during development. *Adv Exp Med*
- 2 *Biol* 717:81-91.
- 3 Le Meur K, Galante M, Angulo MC, Audinat E (2007) Tonic activation of NMDA receptors by ambient
- 4 glutamate of non-synaptic origin in the rat hippocampus. *J Physiol* 580:373-383.
- 5 Lerma J, Marques JM (2013) Kainate receptors in health and disease. *Neuron* 80:292-311.
- 6 Levesque M, Avoli M (2013) The kainic acid model of temporal lobe epilepsy. *Neurosci Biobehav Rev*
- 7 37:2887-2899.
- 8 Liu QS, Xu Q, Arcuino G, Kang J, Nedergaard M (2004) Astrocyte-mediated activation of neuronal kainate
- 9 receptors. *Proc Natl Acad Sci U S A* 101:3172-3177.
- 10 Lysetskiy M, Foldy C, Soltesz I (2005) Long- and short-term plasticity at mossy fiber synapses on mossy
- 11 cells in the rat dentate gyrus. *Hippocampus* 15:691-696.
- 12 Margerison JH, Corsellis JA (1966) Epilepsy and the temporal lobes. A clinical, electroencephalographic
- 13 and neuropathological study of the brain in epilepsy, with particular reference to the temporal
- 14 lobes. *Brain* 89:499-530.
- 15 Matsuda K, Budisantoso T, Mitakidis N, Sugaya Y, Miura E, Kakegawa W, Yamasaki M, Konno K,
- 16 Uchigashima M, Abe M, Watanabe I, Kano M, Watanabe M, Sakimura K, Aricescu AR, Yuzaki M
- 17 (2016) Transsynaptic Modulation of Kainate Receptor Functions by C1q-like Proteins. *Neuron*
- 18 90:752-767.
- 19 Melyan Z, Wheal HV, Lancaster B (2002) Metabotropic-mediated kainate receptor regulation of IsAHP and
- 20 excitability in pyramidal cells. *Neuron* 34:107-114.
- 21 Mulle C, Sailer A, Perez-Otano I, Dickinson-Anson H, Castillo PE, Bureau I, Maron C, Gage FH, Mann JR,
- 22 Bettler B, Heinemann SF (1998) Altered synaptic physiology and reduced susceptibility to kainate-
- 23 induced seizures in GluR6-deficient mice. *Nature* 392:601-605.
- 24 Nicoll RA, Schmitz D (2005) Synaptic plasticity at hippocampal mossy fibre synapses. *Nat Rev Neurosci*
- 25 6:863-876.
- 26 Pabst M, Braganza O, Dannenberg H, Hu W, Pothmann L, Rosen J, Mody I, van Loo K, Deisseroth K, Becker
- 27 AJ, Schoch S, Beck H (2016) Astrocyte Intermediaries of Septal Cholinergic Modulation in the
- 28 Hippocampus. *Neuron* 90:853-865.
- 29 Pajarillo E, Rizer A, Lee J, Aschner M, Lee E (2019) The role of astrocytic glutamate transporters GLT-1 and
- 30 GLAST in neurological disorders: Potential targets for neurotherapeutics. *Neuropharmacology*
- 31 161:107559.
- 32 Pal B (2015) Astrocytic Actions on Extrasynaptic Neuronal Currents. *Front Cell Neurosci* 9:474.
- 33 Patton PE, McNaughton B (1995) Connection matrix of the hippocampal formation: I. The dentate gyrus.
- 34 *Hippocampus* 5:245-286.
- 35 Pinky NF, Wilkie CM, Barnes JR, Parsons MP (2018) Region- and Activity-Dependent Regulation of
- 36 Extracellular Glutamate. *J Neurosci* 38:5351-5366.
- 37 Puighermanal E, Biever A, Espallergues J, Gangarossa G, De Bundel D, Valjent E (2015) *drd2-cre:ribotag*
- 38 mouse line unravels the possible diversity of dopamine d2 receptor-expressing cells of the dorsal
- 39 mouse hippocampus. *Hippocampus* 25:858-875.
- 40 Ratzliff A, Santhakumar V, Howard A, Soltesz I (2002) Mossy cells in epilepsy: rigor mortis or vigor mortis?
- 41 *Trends Neurosci* 25:140-144.
- 42 Ribak CE, Shapiro LA (2007) Ultrastructure and synaptic connectivity of cell types in the adult rat dentate
- 43 gyrus. *Prog Brain Res* 163:155-166.
- 44 Ribak CE, Seress L, Amaral DG (1985) The development, ultrastructure and synaptic connections of the
- 45 mossy cells of the dentate gyrus. *J Neurocytol* 14:835-857.
- 46 Richter KN et al. (2018) Glyoxal as an alternative fixative to formaldehyde in immunostaining and super-
- 47 resolution microscopy. *EMBO J* 37:139-159.

- 1 Robinson JH, Deadwyler SA (1981) Kainic acid produces depolarization of CA3 pyramidal cells in the vitro
- 2 hippocampal slice. *Brain Res* 221:117-127.
- 3 Rose CR, Felix L, Zeug A, Dietrich D, Reiner A, Henneberger C (2017) Astroglial Glutamate Signaling and
- 4 Uptake in the Hippocampus. *Front Mol Neurosci* 10:451.
- 5 Ruiz A, Sachidhanandam S, Utvik JK, Coussen F, Mulle C (2005) Distinct subunits in heteromeric kainate
- 6 receptors mediate ionotropic and metabotropic function at hippocampal mossy fiber synapses. *J*
- 7 *Neurosci* 25:11710-11718.
- 8 Rusina E, Bernard C, Williamson A (2021) The Kainic Acid Models of Temporal Lobe Epilepsy. *eNeuro* 8.
- 9 Scharfman HE (1994) Evidence from simultaneous intracellular recordings in rat hippocampal slices that
- 10 area CA3 pyramidal cells innervate dentate hilar mossy cells. *J Neurophysiol* 72:2167-2180.
- 11 Scharfman HE (2016) The enigmatic mossy cell of the dentate gyrus. *Nat Rev Neurosci* 17:562-575.
- 12 Scharfman HE (2018) Advances in understanding hilar mossy cells of the dentate gyrus. *Cell Tissue Res*
- 13 373:643-652.
- 14 Scharfman HE, Schwartzkroin PA (1988) Electrophysiology of morphologically identified mossy cells of the
- 15 dentate hilus recorded in guinea pig hippocampal slices. *J Neurosci* 8:3812-3821.
- 16 Senzai Y, Buzsaki G (2017) Physiological Properties and Behavioral Correlates of Hippocampal Granule
- 17 Cells and Mossy Cells. *Neuron* 93:691-704 e695.
- 18 Seress L, Abraham H, Horvath Z, Doczi T, Janszky J, Klemm J, Byrne R, Bakay RA (2009) Survival of mossy
- 19 cells of the hippocampal dentate gyrus in humans with mesial temporal lobe epilepsy. *J Neurosurg*
- 20 111:1237-1247.
- 21 Shin JH, Kim YS, Linden DJ (2008) Dendritic glutamate release produces autocrine activation of mGluR1 in
- 22 cerebellar Purkinje cells. *Proc Natl Acad Sci U S A* 105:746-750.
- 23 Sloviter RS, Zappone CA, Harvey BD, Bumanglag AV, Bender RA, Frotscher M (2003) "Dormant basket cell"
- 24 hypothesis revisited: relative vulnerabilities of dentate gyrus mossy cells and inhibitory
- 25 interneurons after hippocampal status epilepticus in the rat. *J Comp Neurol* 459:44-76.
- 26 Straub C, Hunt DL, Yamasaki M, Kim KS, Watanabe M, Castillo PE, Tomita S (2011) Distinct functions of
- 27 kainate receptors in the brain are determined by the auxiliary subunit Neto1. *Nat Neurosci*
- 28 14:866-873.
- 29 Straub C, Noam Y, Nomura T, Yamasaki M, Yan D, Fernandes HB, Zhang P, Howe JR, Watanabe M,
- 30 Contractor A, Tomita S (2016) Distinct Subunit Domains Govern Synaptic Stability and Specificity
- 31 of the Kainate Receptor. *Cell Rep* 16:531-544.
- 32 Takasaki C, Yamasaki M, Uchigashima M, Konno K, Yanagawa Y, Watanabe M (2010) Cytochemical and
- 33 cytological properties of perineuronal oligodendrocytes in the mouse cortex. *Eur J Neurosci*
- 34 32:1326-1336.
- 35 Tamamaki N, Yanagawa Y, Tomioka R, Miyazaki J, Obata K, Kaneko T (2003) Green fluorescent protein
- 36 expression and colocalization with calretinin, parvalbumin, and somatostatin in the GAD67-GFP
- 37 knock-in mouse. *J Comp Neurol* 467:60-79.
- 38 Tomita S, Castillo PE (2012) Neto1 and Neto2: auxiliary subunits that determine key properties of native
- 39 kainate receptors. *J Physiol* 590:2217-2223.
- 40 Wang LY, Taverna FA, Huang XP, MacDonald JF, Hampson DR (1993) Phosphorylation and modulation of
- 41 a kainate receptor (GluR6) by cAMP-dependent protein kinase. *Science* 259:1173-1175.
- 42 Wenzel HJ, Buckmaster PS, Anderson NL, Wenzel ME, Schwartzkroin PA (1997) Ultrastructural localization
- 43 of neurotransmitter immunoreactivity in mossy cell axons and their synaptic targets in the rat
- 44 dentate gyrus. *Hippocampus* 7:559-570.
- 45 Westbrook GL, Lothman EW (1983) Cellular and synaptic basis of kainic acid-induced hippocampal
- 46 epileptiform activity. *Brain Res* 273:97-109.

- 1 Wyeth MS, Pelkey KA, Petralia RS, Salter MW, McInnes RR, McBain CJ (2014) Neto auxiliary protein
2 interactions regulate kainate and NMDA receptor subunit localization at mossy fiber-CA3
3 pyramidal cell synapses. *J Neurosci* 34:622-628.
- 4 Zhu QJ, Kong FS, Xu H, Wang Y, Du CP, Sun CC, Liu Y, Li T, Hou XY (2014) Tyrosine phosphorylation of GluK2
5 up-regulates kainate receptor-mediated responses and downstream signaling after brain
6 ischemia. *Proc Natl Acad Sci U S A* 111:13990-13995.
- 7 Zilberter Y (2000) Dendritic release of glutamate suppresses synaptic inhibition of pyramidal neurons in
8 rat neocortex. *J Physiol* 528:489-496.

9

10

1 **Figure 1. Activation of KARs mediates inward currents in hilar mossy cells.** (A) Identification
2 of hilar mossy cells (MCs) in acute hippocampal slices. *Left*, schematic of MC recordings in the
3 hilus of the dentate gyrus (DG). *Middle*, patched neurons were depolarized to analyze their firing
4 properties. *Right*, post-hoc staining of a MC using Alexa 594-conjugated streptavidin. The yellow
5 boxed area is magnified on the right-hand side. Patched cells were confirmed to be MCs if evoked
6 spikes displayed no evident afterhyperpolarization and by the presence of thorny excrescences
7 (TEs) (white arrowheads). (B) Representative experiment showing that bath application of 0.3
8 and 3 μM kainic acid (KA) in the same cell induced concentration-dependent inward currents in
9 MCs (*top*), but only a negligible inward current in dentate gyrus granule cells (GC) (*bottom*). (C)
10 Summary plot of the amplitude of the inward currents (ΔI holding) induced by KA application. (D)
11 Representative experiments showing that KA-induced inward current was not affected by co-
12 application of TTX (0.5 μM) (*top*) but it was abolished by the AMPAR/KARs antagonist NBQX (25
13 μM) (*bottom*). A low concentration of KA (0.3 μM) was previously tested to verify the presence of
14 a normal, fully reversible KA-induced current in the same cell. (E) Summary plot. (F) KA-induced
15 currents in MCs were robust in WT (*top*) but abolished in *GluK2* KO mice (*bottom*). (G)
16 Concentration-response curve in WT and *GluK2* KO mice. Data are presented as mean \pm S.E.M.

17 **Figure 2. *GluK2*-containing KARs mediate KA-induced robust action potential firing of**
18 **MCs.** (A) *Top*, Effect of of KA bath application (0.3 and 3 μM) on MCs membrane potential in
19 current-clamp configuration. 3 μM KA application induced firing with faster onset and higher
20 frequency than 0.3 μM KA. Firing in 3 μM KA eventually disappeared likely due to excessive
21 depolarization and action potential refractoriness. *Bottom*, average firing rate histogram
22 (expressed as spikes per second) for the experiments in top panel. Black and grey traces
23 represent mean and S.E.M. of MCs firing rate. (B) Representative traces showing no effect of KA
24 application on MCs firing in *GluK2* KO mice.

25 **Figure 3. KAR-mediated transmission at MF-CA3 but not MF-MC synapses.** (A). *Left*, Bath
26 application of the selective AMPAR antagonist GYKI 53655 (30 μM) abolished synaptic
27 transmission at MF-MC synapses. *Right*, representative average traces (30 consecutive
28 responses). (B) Bath application of the mGluR2/3 agonist DCG-IV (1 μM) significantly reduced
29 MF-MC EPSCs ($\sim 70\%$). (C) *Left*, GYKI 53655 application (30 μM) blocked AMPAR-mediated
30 transmission at the MF-CA3 synapse, thus revealing a KAR-mediated component that was
31 blocked by 25 μM NBQX. *Middle*, representative average traces (30 consecutive responses)
32 before and after GYKI application, and after subsequent application of NBQX. *Right*, normalized
33 AMPAR and KAR components highlighting the slow kinetics of the KAR-EPSC. In all traces

1 included in this figure, stimulus artifacts were deleted for clarity. Data are presented as mean \pm
2 S.E.M.

3

4 **Figure 4. Contrasting localization of GluK2/3 and its molecular partners in CA3 stratum**
5 **lucidum and DG hilus. (A,B)** In WT mice, GluK2/3 labeling is intense in CA3 *stratum lucidum*,
6 while it is moderate and diffuse in the dentate gyrus (A). Note the lack of GluK2/3 staining in
7 *GluK2* KO mice, indicating the specificity of the GluK2/3 antibody and exclusive expression of
8 GluK2 in these hippocampal regions (B). **(C)** Quadplex immunofluorescence for GFP (C₁, white),
9 calretinin (C₂, blue), GluK2/3 (C₄, red), and PSD95 (C₅, green) in *GAD67^{+GFP}* mice. **(D)** Double
10 immunofluorescence for GluK2/3 (D₁, red) and Neto1 (D₂, green). Note that intense signal for
11 Neto 1 is almost limited to CA3 *stratum lucidum*. **(E-H)** Distinct GluK2/3 and PSD95 localization
12 between CA3 pyramidal cells and hilar MCs. **(E,F)** GluK2/3 and PSD95 labeling are intense in
13 the CA3 *stratum lucidum* (E). A high-magnification image confirms their extensive overlap (F).
14 **(G,H)** A MC, which is identified as a calretinin-positive (G₁, blue) and GFP-negative (G₂, white) cell
15 in *GAD67^{+GFP}* mice, shows weak labeling for GluK2/3 on its dendrites (red, arrows in H). Note
16 that such GluK2/3 puncta are neither overlapped nor associated with PSD95 signal (H₂, green).
17 **(I-L)** Distinct GluK2/3 and Neto1 localization between CA3 pyramidal cells and hilar MCs. **(I,J)**
18 Intense GluK2/3 and Neto1 labeling in the CA3 *stratum lucidum* (I). A high-magnification image
19 shows Neto1 labeling is only observed on GluK2/3-positive puncta (J). **(K,L)** A MC shows weak
20 labeling for GluK2/3 on its dendrites (red, arrows in L) but lacks Neto1 labeling (L₂, green). DG,
21 dentate gyrus; GrDG, granule cell layer of the DG; MoDG, molecular layer of the DG; SL, *stratum*
22 *lucidum*; SP, *stratum pyramidale*; SR, *stratum radiatum*. Scale bars, **(A,D)** 100 μ m; **(E,F,I,J,G,K)**
23 10 μ m; **(H,L)** 2 μ m.

24

25 **Figure 5. GluK2/3 in hilar MCs are enriched at non-synaptic sites. (A,B)** A large MF terminal
26 characteristically forms multiple asymmetric synapses (arrowheads) with TEs (blue) of CA3
27 pyramidal cells. In wild-type (WT) mice, metal particles for GluK2/3 (arrows) are prevalent on PSD
28 (A). Postsynaptic labeling is absent in *GluK2* KO mouse (B). **(C-F)** MCs (green) contact with large
29 MF terminals in the hilus of the DG. In WT mice, MF synapses on MC spines are rarely labeled
30 for GluK2/3; occasionally, non-synaptic membrane on dendritic shaft has low but significant
31 labeling (C). Neither synaptic nor extrasynaptic labeling is observed in *GluK2* KO mice (D). MCs
32 occasionally have thin dendrites originating from soma (E) and contact with large MF terminal via

1 multiple spines (F). Note that metal particle for GluK2/3 (arrows) leave postsynaptic membrane
2 unlabeled. (G) Average and individual data points for the density of metal particles for GluK2/3
3 on CA3 pyramidal cells (*blue symbols, left axis*) and hilar MCs (*green symbols, right axis*). Note
4 low but significant non-synaptic labeling on MCs. Edges of PSD are indicated by pairs of
5 arrowheads. Number of measured profiles (#) and membrane length (mm) are indicated in
6 parentheses. Dunn's post Test. * $p < 0.05$; ** $p < 0.01$; *** $p < 0.001$. Scale bars, (A-D,F) 200 nm;
7 (E) 1 μ m.

8

9 **Fig 6. MC-KARs can be activated by endogenous glutamate.** (A) Representative experiments
10 showing the effect of TBOA (100 μ M - *left*), dihydrokainic acid (DHK 100 μ M – *middle*) mice and
11 DHK in *GluK2* KO mice on MCs holding current. Recordings conditions were as in Fig.1. Activation
12 of KARs was confirmed by application of the AMPAR/KAR antagonist NBQX (25 μ M) at the end
13 of the recording. NBQX was not applied in *GluK2* KO as no inward current was detected. (B)
14 Quantification of the effect of TBOA (*left*) and DHK (*right*) on MCs holding current. Dots represent
15 the average current of 2 minutes of recording taken 2 minutes before DHK/TBOA application
16 (baseline), 2 minutes before NBQX application (+DHK/TBOA), and 2 minutes at the end of NBQX
17 application (+NBQX). Connected dots represent the same cell. (C) Summary plot of the
18 experiments shown in (B) and in the DHK *GluK2* KO dataset. (TBOA: 61.24 ± 18.61 pA; * $p =$
19 0.02173 one sample t Test; DHK: 28.06 ± 7.4 pA; $n = 3a/6c$; $n = 4a/6c$; DHK *GluK2* KO: $-8.5 \pm$
20 7.47 ; $n = 3a/4c$; DHK vs DHK *GluK2* KO mice: * $p = 0.0105$ two sample t Test). Data are presented
21 as mean \pm S.E.M.

22

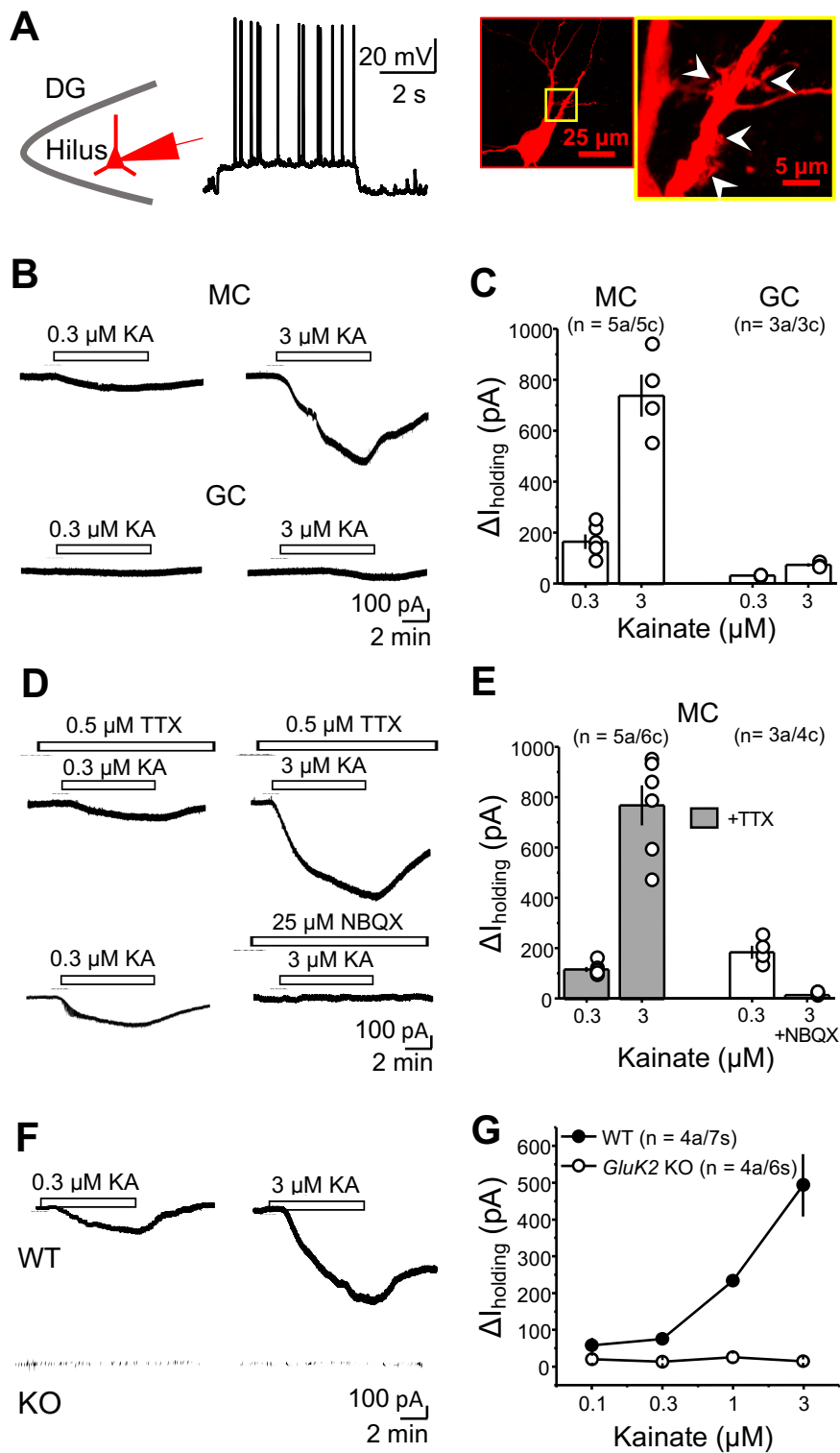


Figure 1

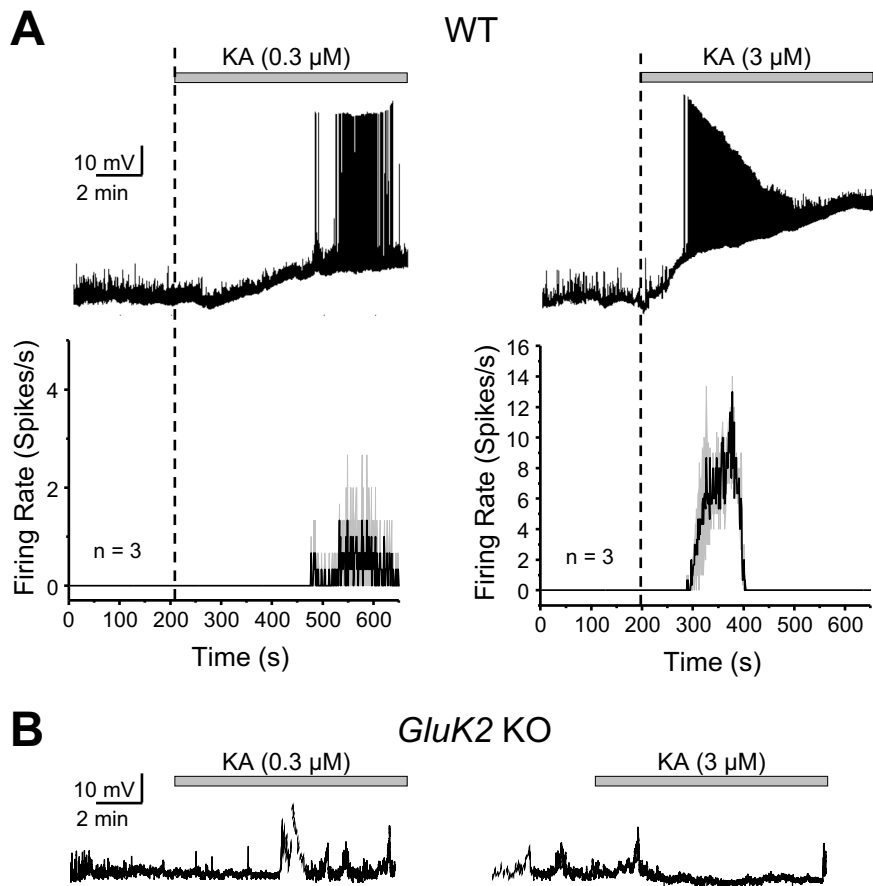


Figure 2

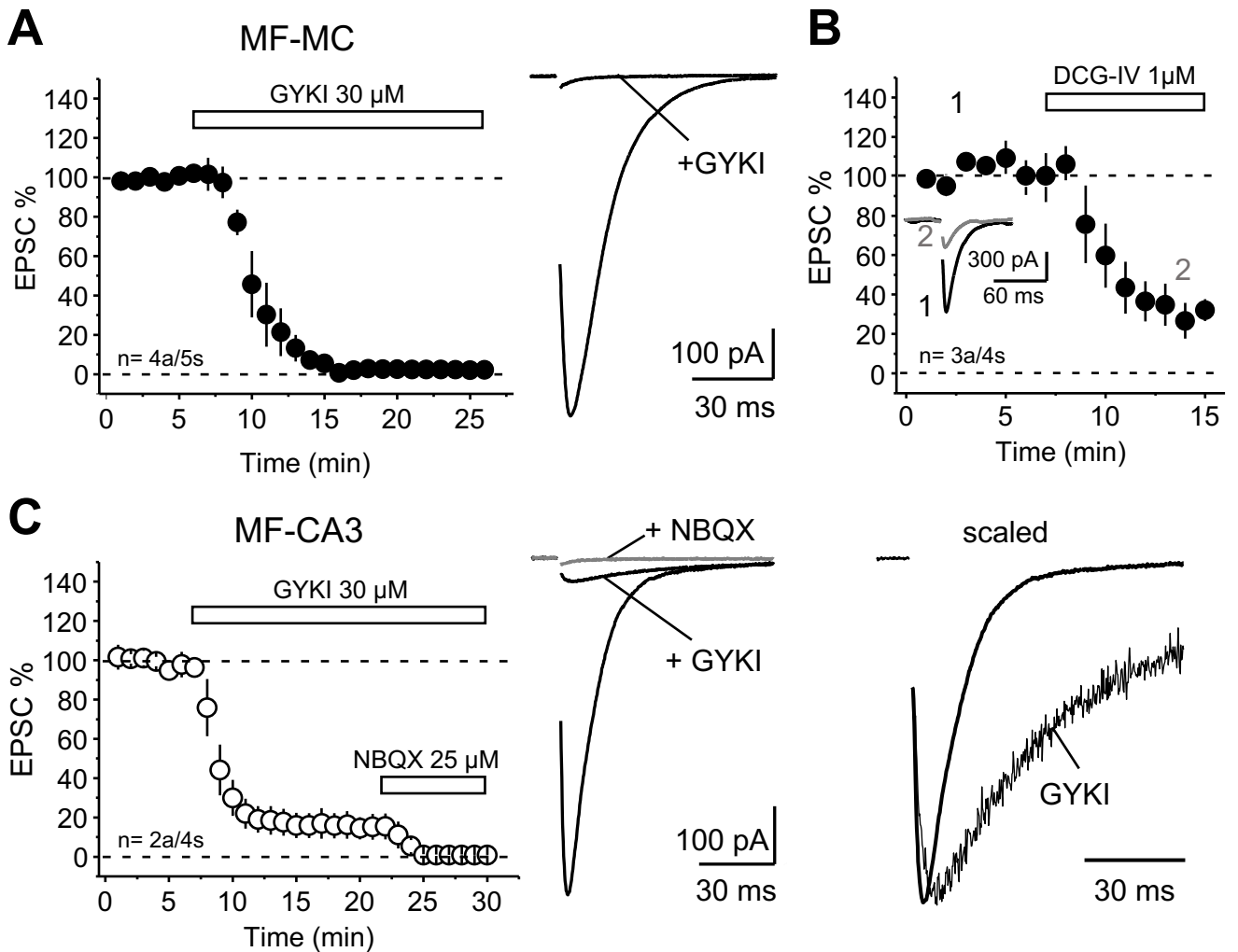


Figure 3

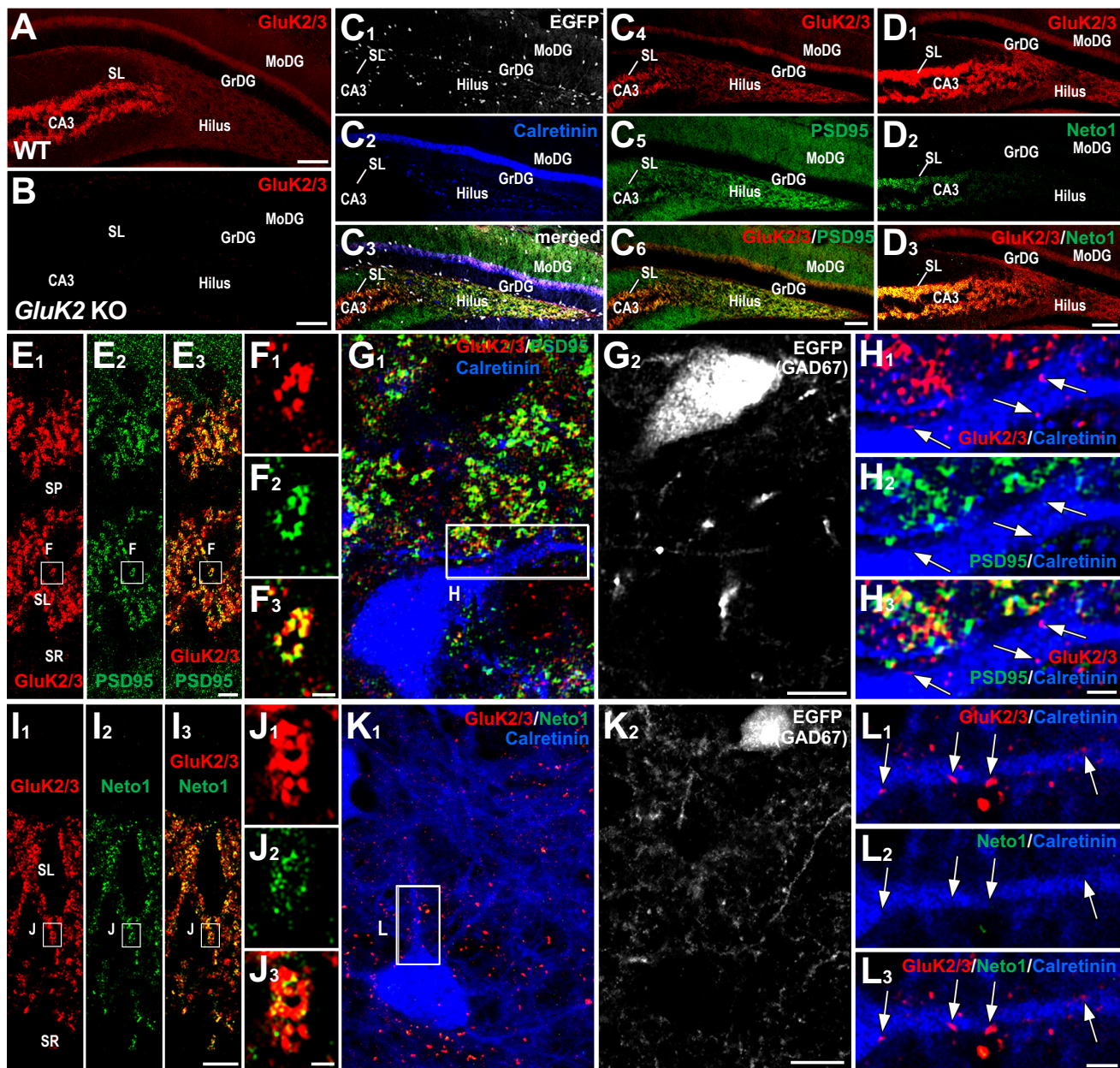


Figure 4

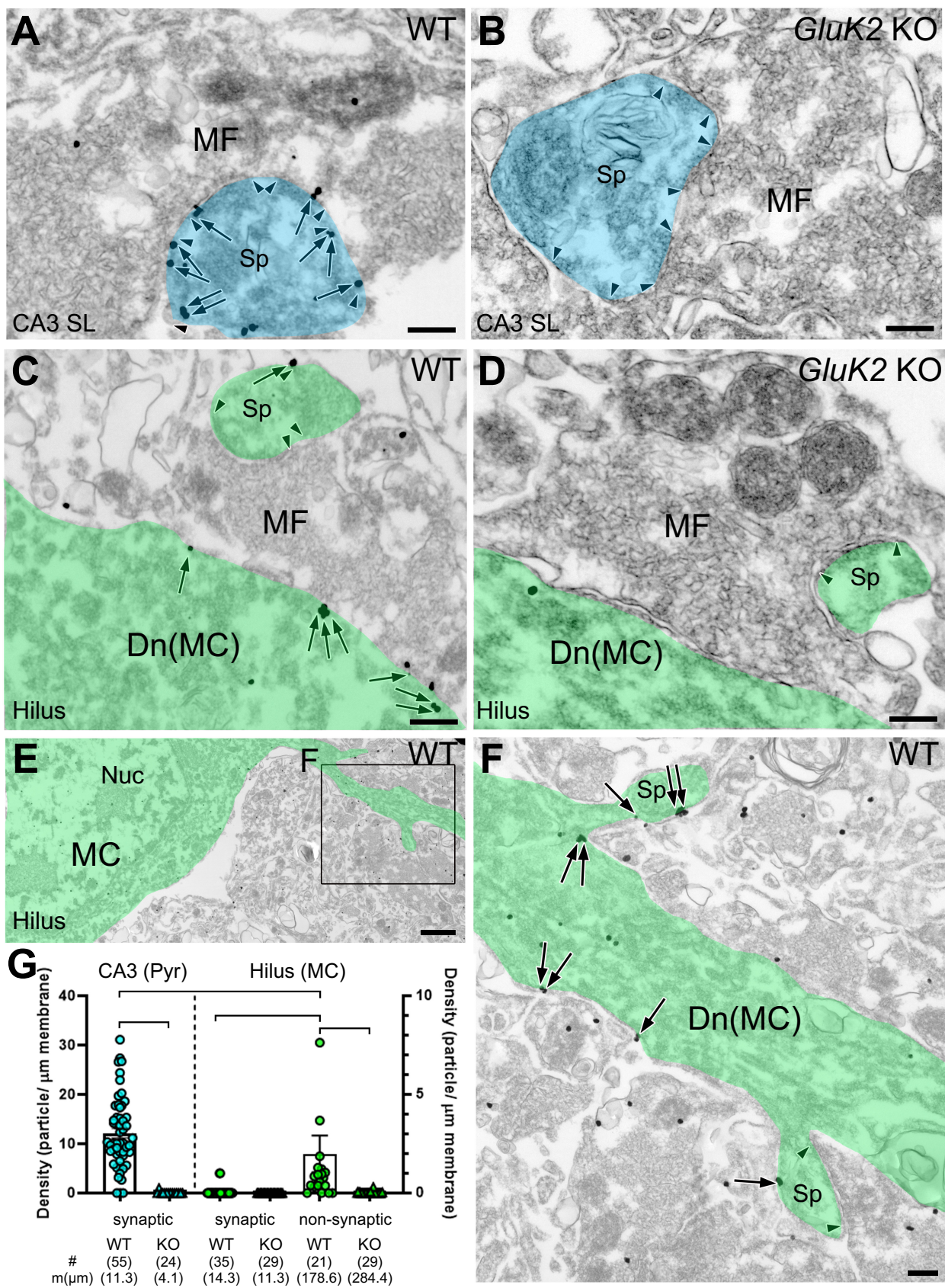


Figure 5

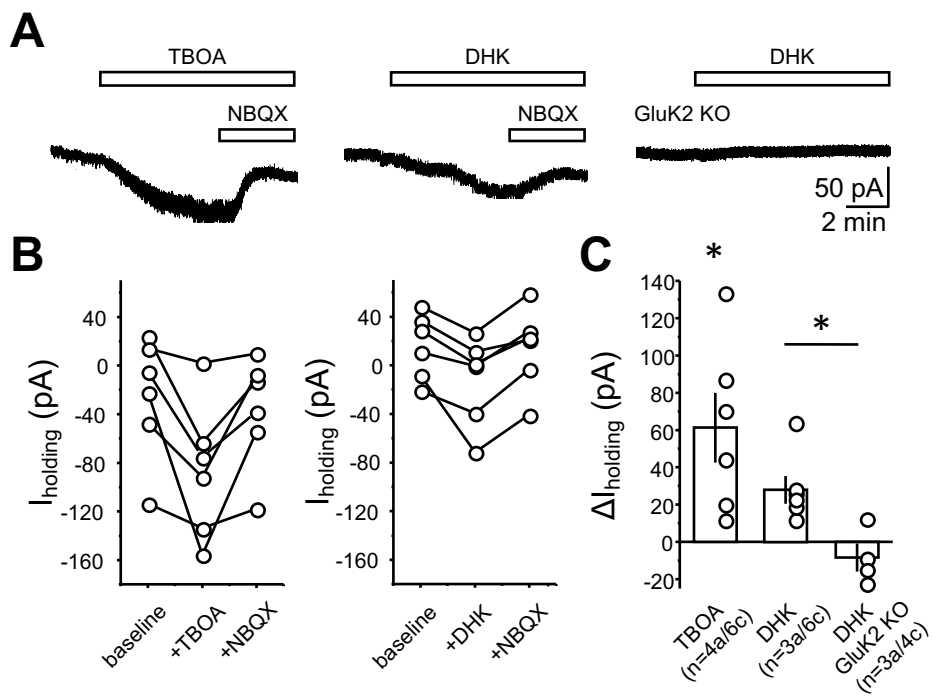


Figure 6